FULL PAPER

DPhG ARCH PHARM
Archiv der Pharmazie

Novel benzo[b]xanthene derivatives: Bismuth(III) triflate-catalyzed one-pot synthesis, characterization, and acetylcholinesterase, glutathione S-transferase, and butyrylcholinesterase inhibitory properties

Kadir Turhan[1] | Begüm Pektaş[1] | Fikret Türkan[2] | Fatma T. Tuğcu[1] | Zuhal Turgut[1] | Parham Taslimi[3] | Halide S. Karaman[4] | Ilhami Gulcin[4]

[1]Department of Chemistry, Faculty of Art and Sciences, Davutpasa Campus, Yildiz Technical University, Istanbul, Turkey

[2]Department of Medical Services and Techniques, Vocational School of Health Services, Igdir University, Iğdır, Turkey

[3]Department of Biotechnology, Faculty of Science, Bartin University, Bartin, Turkey

[4]Department of Chemistry, Faculty of Science, Ataturk University, Erzurum, Turkey

Correspondence
Kadir Turhan, Department of Chemistry, Faculty of Art and Sciences, Davutpasa Campus, Yildiz Technical University, 34210 Istanbul, Turkey.
Email: kturhan@yildiz.edu.tr

Funding information
Yildiz Teknik Üniversitesi, Grant/Award Number: FYL-2017-3243

Abstract

In this study, 3,4-dihydro-12-aryl-1H-benzo[b]xanthene-1,6,11-(2H,12H)trione compounds were obtained through one-pot condensation of various substituted aromatic aldehydes, 2-hydroxy-1,4-naphthoquinone, and dimedone in the presence of $Bi(OTf)_3$ as a green and reusable catalyst. The structural characterization of these novel substituted benzo[b]xanthenes was performed by spectroscopic methods, and their inhibitory actions against butyrylcholinesterase (BChE), acetylcholinesterase (AChE), and glutathione S-transferase (GST) were investigated. GST is an enzyme responsible for removing toxic molecules during Phase II reactions in the detoxification mechanism. The AChE and BChE enzymes, which are called cholinesterases, are among the enzymes that occur especially during dementia such as brain damage or Alzheimer's disease. Inhibition effects of the benzo[b]xanthene derivatives on AChE, BChE, and GST were found at the millimolar level. The best inhibitor for GST is compound **4a** (31.18 ± 6.13 mM), for AChE, it is compound **4d** (28.16 ± 3.46 mM), and for BChE, it is compound **4f** (36.24 ± 3.19 mM). Compound **4a** inhibited the dimerization of GST subunits, and compounds **4d** and **4f** directly inhibited the catalytic activity by interacting with the catalytic active site or a related site of the AChE and BChE enzymes, respectively.

KEYWORDS
acetylcholinesterase, enzyme inhibition, molecular docking, spectrophotometry, synthesis

1 | INTRODUCTION

Benzoxanthenes are tetracyclic dibenzopyrans with diverse biological and therapeutic properties such as antibacterial, antiviral, antiinflammatory, antitumor, antimalarial, and pesticidal activities.[1–9] These heterocyclic compounds, also known as leuco dyes that are pH-sensitive fluorescent materials, can be used in photodynamic therapy, polymer photo imaging systems, and laser technologies due to the fluorescence activities of the naphthoquinone nucleus.[10–15]

Despite continued research efforts toward the development of anticancer drugs, cancer remains a primary cause of death. It is well established that small heterocyclic molecules are the predominant building blocks for biologically active compounds. Xanthene, one of these building blocks, is an important structural unit commonly found in natural products. Molecular scaffolds of xanthene are important as PIM1 kinase inhibitors. Epicalyx is the most potent member of this class as an anticancer agent against human HT-1080 fibrosarcoma and murine 26-L5 carcinoma.[16,17]

In recent decades, the development of a faster and more efficient synthesis of heterocyclic compounds containing xanthene and benzoxanthene scaffolds in their structures has attracted considerable attention. A number of methodologies for the synthesis of these compounds have been reported, which include various catalysts, such as aqueous systems[14,16,18,19], P_2O_5,[17] DABCO-based ionic liquid,[20] [NMP]H_2PO_4,[21] LiCl,[22] Fe_3O_4 nanoparticles,[23] nano-Fe_3O_4/PEG/succinic anhydride,[24] poly(4-vinyl-pyridinium) hydrogen sulfate,[25] nanocatalytic Zn/MCM-41-SO$_3$H,[26] CuSO$_4$·5H$_2$O,[27] GaCl$_3$,[28] AlHMS,[29] LPCAS,[30] tetrapropylammonium bromide,[31] H-zeolite,[32] STA,[33] and various ionic liquids.[34–36] However, most of the catalysts in question have led researchers to search for different catalysts, as they have one or more drawbacks, such as being uneconomical and useless methods, and carrying out the reaction with lower yields.

Trifluoromethanesulfonic acids, which can be considered as superacids, are one of the most acidic monoprotic organic acids, which easily form metal triflates on reaction with most metals. In the last few years, bismuth(III) triflate (Bi(OTf)$_3$) has been reported as a new and an effective catalyst. Bismuth(III) compounds showing Lewis acidity due to poor protection of 4f electrons (lanthanide shrinkage) have attracted great attention due to their low toxicity, low costs, ease of use, high catalytic efficiency, and stability. Bismuth compounds are also versatile reagents for the synthesis of pharmaceutically interesting compounds and various organic reactions involving the synthesis of natural products.[37–40]

The multicomponent reactions are useful methods in which three or more reactants are combined in a single chemical step, to produce products containing significant portions of all reactants. Reactions in one pot are effective in forming highly functionalized small organic molecules, which can be obtained in a single step from readily available starting materials. In these reactions, diversity, time, labor, cost, and waste products are minimized.[13–17,41]

Glutathione S-transferase (GST; E.C.2.5.1.18) is a multifunctional enzyme that catalyzes the first step formation of mercapturic acid that occurs as a final product in the detoxification metabolic process.[42,43] GST enzyme is present in the liver of mammals such as humans, rats, and mice.[43,44] Additionally, GSTs are present in plants, fungi, insects, and bacteria.[44–47] Mitochondrial, cytosolic, and microsomal enzymes are GSTs' derivatives, and these enzymes metabolize various electrophilic compounds via a reduced glutathione conjugation.[48,49]

Acetylcholinesterase (AChE) and butyrylcholinesterase (BChE) enzymes are both expressed as cholinesterases and are very important enzymes that break down acetylcholine (ACh) into acetate and other choline and some other choline ester molecules that function as neurotransmitter molecules, which are considered as drugs for Alzheimer's disease (AD).[50–52] AChE inhibitors can be used as a therapeutic for some common diseases including AD. Therefore, these inhibitors have been used in the treatment of some traumatic disorders such as AD, myasthenia gravis, and glaucoma. In addition, cholinesterase inhibitors are extensively utilized as pesticides and, if misused, can produce toxic responses in humans and mammals.[53–55]

The aim of this study was to investigate the inhibition effects of benzo[b]xanthane derivatives, which were synthesized in the presence of a catalytic amount of Bi(OTf)$_3$, for the first time. The compounds were tested against some metabolic enzymes including AChE, BChE, and GST enzymes, applying in vitro conditions. Inhibitors of AChE and BChE enzymes are very important in the use of AD drugs. GST inhibitors are emerging as promising therapeutic agents for managing the development of resistance amongst anticancer agents. In the field of diagnostic medicine, as well as in antiparasitic drug development, GST inhibitors are important lead molecules.

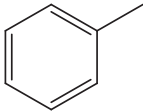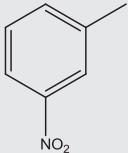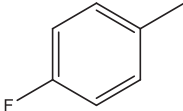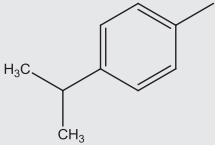## 2 | RESULTS AND DISCUSSION

2.1 | Chemistry
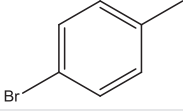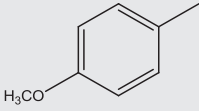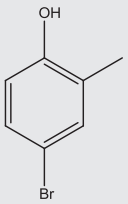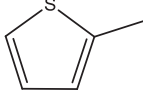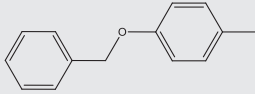
In this report, the three-component, one-pot condensation of lawsone (2-hydroxy-1,4-naphthoquinone), dimedone (5,5-dimethyl-1,3-cyclohexanedione), and aromatic aldehyde was studied in the presence of the Bi(OTf)$_3$ catalyst for the preparation of 3,3-dimethyl-12-aryl-3, 4-dihydro-1H-benzo[b]xanthene-1,6,11-(2H,12H)triones (Scheme 1 and Table 1). Bi(OTf)$_3$ catalyst is first tried in this study in such compound synthesis. In this study, 10 substances (4a–j) were synthesized. Compounds 4h–j were not found in the literature.
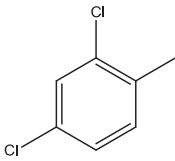
Initially, to optimize the catalytic system, we examined the effect of the catalyst amount on the model reaction (Table 2).
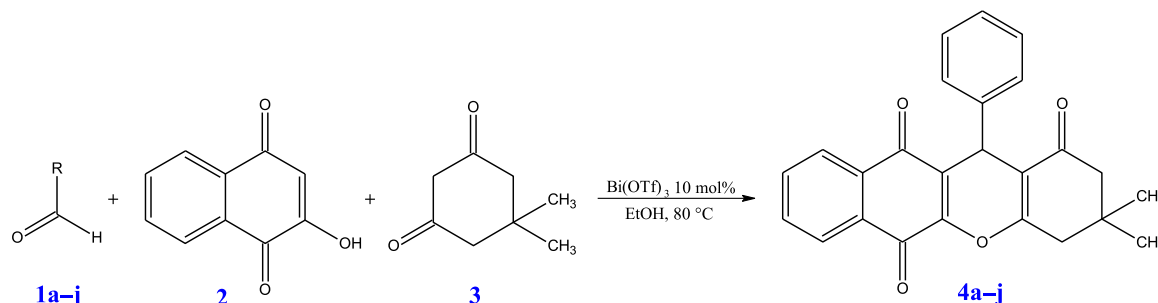
SCHEME 1 The one-pot synthesis of benzo[b]xanthene derivatives. Bi(OTf)$_3$, bismuth(III) triflate; EtOH, ethyl alcohol

TABLE 1 Bismuth(III) triflate-catalyzed one-pot synthesis of benzo[b]xanthene derivatives

Entry	Compounds	R	M.p. (°C)	Yield (%)
1	4a		263–264[9,11,13,18,20,35,37,41]	
2	4b		236–237[11,13,18,35,41,42]	88
3	4c		246–247[11,14,18,20,42]	92
4	4d		222–225[25]	85
5	4e		270–271[11,20,35]	86
6	4f		241–242[35]	84
7	4g		256–257[13]	89
8	4h		249–251	81
9	4i		232–233	82
10	4j		253–254	80

Spectroscopic methods were used to elucidate the structures of all synthesized compounds. The peaks observed between 1,682 and 1,651 cm^{-1} indicate the C=O stress, and the peaks formed between 3,071 and 3,000 cm^{-1} reveal the aromatic structure when the Fourier-transform infrared (FTIR) spectra are observed to clarify the structures of the compounds obtained with analytical purity. In addition, the singlets observed around 0.94–1.05 ppm in the ^{1}H nuclear magnetic resonance (NMR) spectra belong to dimedone molecule's CH$_3$ (methyl) protons and the peaks observed around 2.15–2.45 ppm belong to dimedone ring's CH$_2$ (methylene) protons. The CH proton, to which the aromatic aldehyde is added to the ring, is observed around 5 ppm. In addition, aromatic protons of 2-hydroxynaphthalene-1,4-dione and

TABLE 2 Effects of the catalyst amount on the reaction yield

Entry	Catalyst	Solvent	Temperature/time	Reaction medium/yield
1	Bi(OTf)$_3$, 10 mol%	EtOH	80°C/6 hr	One-pot, reflux/89%
2	Bi(OTf)$_3$, 20 mol %	EtOH	80°C/6 hr	One-pot, reflux/84%
3	Bi(OTf)$_3$, 30 mol %	EtOH	80°C/6 hr	One-pot, reflux/85%

Abbreviations: Bi(OTf)$_3$, bismuth(III) triflate; EtOH, ethyl alcohol.

substituted benzaldehyde compounds involved in the formation of the ring (**4a–j**) are observed at 7.56–7.80 and 8.15–8.37 ppm.

We showed the possible reaction mechanism obtained from the literature research on the general reaction equation.[13,18,43,44] Bi(OTf)$_3$ can activate the carbonyl groups of aldehyde **1** to decrease the energy of transition state. Initially, there was Knoevenagel condensation of aryl aldehydes and dimedone (1,3-dicarbonyl compound; **3**), to form 2-[(aryl)methylene]-5,5-dimethylcyclohexane-1,3-dione (**5**). This was followed by Michael addition of 2-hydroxy-1,4-naphthoquinones **2** to **5**. An intermediate form (**6**) was furnished. By keto–enol tautomerization, intramolecular cyclization and dehydration gave the fused-ring compound 3,3-dimethyl-3,4-dihydro-12-aryl-2,3,4,12-tetrahydrobenzo [*b*]xanthene-1,6,11-trione (**4a–j**; Scheme 2).

2.2 | Enzyme inhibition results

2.2.1 | Cholinesterases inhibition results

All novel benzo[*b*]xanthane derivatives (**4a–j**) exhibited a significantly higher AChE inhibitory activity than that of standard AChE inhibitors such as tacrine. Furthermore, the K_i values of these compounds and standard compound (tacrine) are summarized in Table 3. As can be seen from the results obtained in Table 3, these compounds effectively inhibited AChE, with K_i values in the range of 28.16 ± 3.46 to 128.14 ± 21.23 mM. However, all compounds had almost similar inhibition profiles. The most active compound **4d** showed K_i value of 28.16 ± 3.46 mM. For AChE, IC$_{50}$ values of tacrine as a positive control and novel derivatives are expressed in the following order: **4d** (23.31 mM; r^2: 0.9845) < **4f** (27.36 mM; r^2: 0.9763) < **4a** (49.76 mM; r^2: 0.9547) < **4g** (64.32 mM; r^2: 0.9685) < tacrine (116.02 mM; r^2: 0.9783). For BChE, IC$_{50}$ values of TAC as a positive control of some novel benzo[*b*]xanthane derivatives (**4a–j**) are expressed in the following order: **4f** (29.67 mM; r^2: 0.9614) < **4a** (34.56 mM; r^2: 0.9761) < **4b** (36.11 mM; r^2: 0.9859) < **4d** (36.58 mM; r^2: 0.9487) < TAC (125.44mM; r^2: 0.9815). Additionally, the novel benzo[*b*]xanthane derivatives (**4a–j**) effectively inhibited BChE, with K_i values in the range of 36.24 ± 3.19 to 69.25 ± 14.44 mM. However, all these compounds had almost similar inhibition profiles. The most active compound **4f** showed K_i value of 36.24 ± 3.19 mM. In the past decade, efforts in the development of therapy for AD have focused on improving the cholinergic neurotransmission in the brain cells. This mechanism is largely based on the cholinergic hypothesis, which has prompted evaluations on cholinesterase enzyme inhibitors (ChEIs) that increase the central cholinergic neurotransmission by inhibiting ACh degradation. Indeed, ChEI is currently considered as
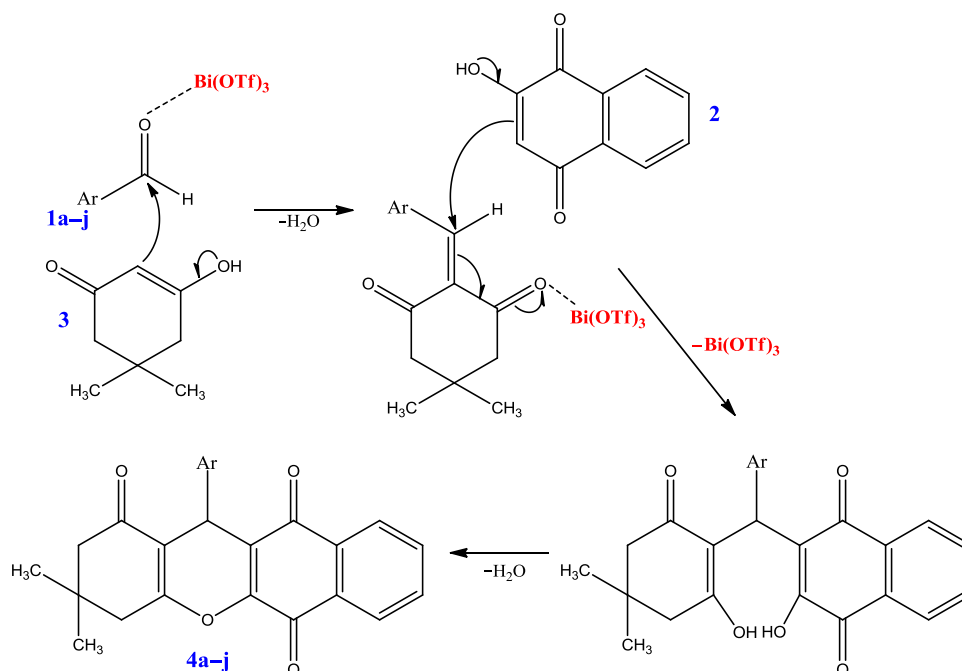
SCHEME 2 The plausible mechanism for the preparation of compound **4**. Bi(OTf)$_3$, bismuth(III) triflate

TABLE 3 Inhibition results of novel benzo[*b*]xanthane derivatives (**4a–j**)

| Molecules | IC$_{50}$ (mM) | | | | | | K_i (mM) | | |
	GST	r^2	AChE	r^2	BChE	r^2	GST	AChE	BChE
4a	28.14	.9652	49.76	.9547	34.56	.9761	**31.18 ± 6.13**	68.47 ± 14.12	39.14 ± 5.66
4b	42.34	.9756	101.56	.9658	36.11	.9859	58.69 ± 11.32	128.14 ± 21.23	48.56 ± 10.94
4c	44.26	.9512	66.84	.9814	41.36	.9587	49.66 ± 9.27	84.21 ± 16.24	44.28 ± 6.28
4d	42.48	.9825	23.31	.9845	36.58	.9487	45.69 ± 7.32	**28.16 ± 3.46**	47.63 ± 6.24
4e	16.25	.9841	78.58	.9769	38.15	.9851	43.38 ± 10.24	102.25 ± 19.43	51.65 ± 13.02
4f	58.45	.9645	27.36	.9763	29.67	.9614	66.12 ± 13.89	38.41 ± 6.33	**36.24 ± 3.19**
4g	51.28	.9785	64.32	.9685	44.45	.9617	66.23 ± 9.22	74.38 ± 10.42	52.16 ± 8.42
4i	31.71	.9687	77.12	.9712	54.84	.9639	51.16 ± 8.42	81.42 ± 11.16	69.25 ± 14.44
4j	48.35	.9618	73.64	.9728	42.82	.9591	50.12 ± 9.14	79.46 ± 12.38	41.68 ± 6.66
TAC	–	–	116.02	.9783	125.44	.9815	–	92.34 ± 28.12	103.28 ± 11.26

Note: Molecules showing the best inhibition for each enzyme are shown in bold.
Abbreviations: AChE, acetylcholinesterase; BChE, butyrylcholinesterase; GST, glutathione S-transferase.

the most promising therapy for AD, because ChEIs re-establish the cholinergic function in human cells by enhancing the ACh amounts in the central neural system.[51,53]

2.2.2 | GST enzyme results

For GST enzyme, novel benzo[*b*]xanthane derivatives (**4a–j**) have IC$_{50}$ values in the range of 16.25–58.45 mM and K_i values in the range of 31.18 ± 6.13 to 66.23 ± 9.22 mM (Table 3). The results have clearly documented that all of these derivatives have shown the inhibitory effects on GST. In fact, the most effective K_i values of compounds **4a** and **4e** were 31.18 ± 6.13 and 43.38 ± 10.24 mM, respectively. For GST, IC$_{50}$ values for novel derivatives are expressed in the following order: ethacrynic acid (EA; [2,3-dichloro-4-(2-methylenebutyryl)phenoxy]acetic acid) as standard (0.01037 mM)[56] < **4e** (16.25 mM; r^2: 0.9841) < **4a** (28.14 mM; r^2: 0.9652) < **4i** (31.71 mM; r^2: 0.9687) < **4b** (42.34 mM; r^2: 0.9756) < **4d** (42.48 mM; r^2: 0.9825). GSTs had crucial effects in the stage II as detoxifying enzymes that act on cytotoxic substances and dissolve them in water and easily from the body. Many tumor cells tend to dramatically increase GST expression, which is associated with a poor prognosis in response to patients' anticancer treatment. The inhibition of elevated GST levels in cells by the chronic esteric acid inhibitor enhances the toxicity of several cancer drugs against cell lines.[57] In a former study, newly synthesized 2-substituted-5-(4-trifluoromethyl phenyl sulfonamido)benzoxazole derivatives were examined for their inhibitory effects on hGST P1-1 enzyme. According to enzyme inhibition studies, most of the tested compounds, showed a better inhibitory activity than the reference drug EA.[58] Recently, some studies reported some sulfonamidobenzoxazole derivatives, which exhibit hGST P1-1 enzyme inhibitory activities, and one of these compounds showed a potency similar to the reference drug EA.[59,60] In this study, the results

of the compounds were poor, compared with the EA as standard, but overall the results were good and inhibition was observed.

2.3 | Molecular docking results

To understand the possible inhibition mechanism of most effective compounds, molecular docking studies were carried out. First, drug-likeness properties of synthesized compounds were calculated, and the properties are presented in Table 4. According to these scores, all compounds were compatible with Lipinski's rule,[61] because the compounds have a molecular weight <500 kDa, hydrogen bond donors and octanol/water partition coefficients <5, and hydrogen bond acceptors <10. The compound was also nontoxic and non-HERG blocker due to its reactive group and blockage of HERG K$^+$ channels. Moreover, all compounds, except **4b**, demonstrated excellent oral absorption and good membrane permeability. The properties of drug similarity have shown that the compounds are favorable to accept as a drug.

Binding sites of the prepared enzymes were predicted and their site scores were calculated. The scores were used to detect catalytically active site, and the binding site with the highest site score was accepted as a catalytically active site. The binding sites and catalytically active sites were used for the assessment of docking hits.

The induced-fit docking method was tested by docking the co-crystallized ligand of the enzyme before the compounds were docked, and the results of the tests were analyzed by root mean square deviation (RMSD) values between the cocrystallized and redocked ligands. According to the results, the ligands have 0.742, 0.106, and 2.714 Å of RMSD values. The values have demonstrated that the cocrystallized and redocked ligands are closely located in the catalytically active site of the enzyme, as seen in Figure 1.

TABLE 4 The drug-likeness properties of the novel benzo[*b*]xanthene derivatives

Compound	rtvFG[a]	MW[b]	DHB[c]	AHB[d]	logPo/w[e]	logHERG[f]	Caco[g]	logBB[h]	PMDCK[i]	% Hum. oral abs.[j]
4a	0	384.431	0	6.50	3.392	−5.519	855.638	−0.475	417.988	100.000
4b	0	429.428	0	7.50	2.648	−5.428	102.458	−1.493	42.157	78.437
4c	0	402.421	0	6.50	3.603	−5.359	868.986	−0.359	767.150	100.000
4d	0	426.511	0	6.50	4.390	−5.683	847.371	−0.627	413.625	100.000
4e	0	463.327	0	6.50	3.955	−5.498	863.772	−0.314	1118.988	100.000
4f	0	414.457	0	7.25	3.438	−5.505	847.061	−0.579	413.461	100.000
4g	0	453.321	0	6.50	4.329	−5.297	1039.441	−0.113	2335.290	100.000
4h	0	479.326	1	7.25	3.755	−5.348	567.706	−0.543	711.255	100.000
4i	0	390.453	0	6.50	3.225	−5.480	670.474	−0.542	430.366	96.414
4j	0	490.554	0	7.25	5.341	−7.342	835.844	−0.858	407.546	100.000

Abbreviation: PMDCK, Predicted apparent Madin–Darby canine kidney.
[a]Reactive group (toxicity).
[b]Molecular weight.
[c]Number of hydrogen bond donors.
[d]Number of hydrogen bond acceptors.
[e]Octanol/water partition coefficient.
[f]IC$_{50}$ value for blockage of HERG K$^+$ channels.
[g]Caco-2 cell membrane permeability.
[h]Brain/blood partition coefficient.
[i]MDCK cell permeability in nm/s.
[j]Qualitative human oral absorption.

The values have also indicated that the docking methods were very reliable. Then, **4a** was docked into the allosteric site of GSH enzyme due to noncompetitive inhibition, and **4d** and **4f** were docked into the catalytically active site of the AChE and BChE enzymes, respectively. The compounds demonstrated a good binding affinity against the enzyme. Their binding affinity is presented in Table 5. The binding affinities were compatible with existing in vitro results on a large scale.

Furthermore, to understand possible inhibition mechanisms of the molecules, their poses with best binding affinity were chosen as the best poses, and the best poses were analyzed on the bases of interactions with enzyme. Compound **4a**, which docked into an allosteric site of GST, formed hydrogen bonds with Arg74 and Gln83 residues of the B subunit. In addition to this, it constructed π–cation and π–π stacking interactions with Arg74 residue of the A subunit

and Try79 residue of the B subunit, respectively (Figures 2a and 3a). The size of the allosteric sites was pretty small; therefore, compound **4a**, which was the smallest and had minimum functional groups among the ligands, was easily located in the site. GST has two types of ligand-binding sites including G-site and H-site. Whereas the G-site bound GSH, H-site bound various compounds such as 1-chloro-2,4-dinitrobenzene (CDNB).[62] The sites play a key role in enzyme catalysis. Besides these sites, the enzyme has a dimerization site, which is necessary for its activity.[63] Huang et al.[64] have indicated that an electrostatic interaction between Arg70, Arg74, Asp90, and Asp94 residues is quite important for dimerization and mutation of the residues causing a loss in the catalytic activity. Our result has shown that compound **4a** caused enzyme inhibition by blocking subunit dimerization.
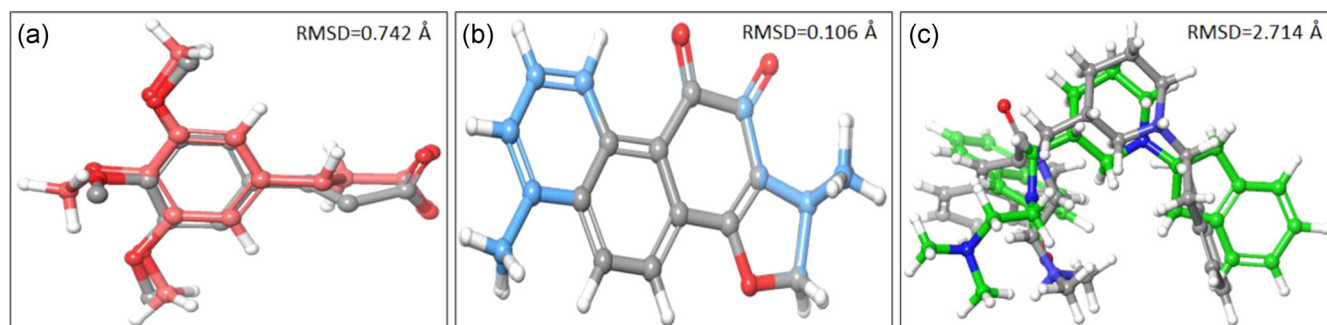
FIGURE 1 The docking methodology reliability test. (a) 3LF, (b) 1YL, and (c) 92H. The cocrystallized ligands are represented in pink, blue, and green ball-and-stick models, respectively. The best pose of redocked ligands is represented as gray ball-and-stick model

TABLE 5 Binding affinity scores of the most effective novel benzo[*b*]xanthene derivatives

Com-pounds	Docking scores (kcal/mol)		
	GST	AChE	BChE
4a	−5.897	–	–
4d	–	−11.257	–
4f	–	–	−10.094

Abbreviations: AChE, acetylcholinesterase; BChE, butyrylcholinesterase; GST, glutathione S-transferase.

Compound **4d** directly formed hydrogen bonds with Phe295 residue and indirectly formed hydrogen bond with Tyr72 and Ser293 residues through a water bridge. The molecule also formed π–π stacking interactions with Trp286 and Tyr341 residues, as seen in Figure 2b. Moreover, it formed an aromatic hydrogen bond with a Tyr341 residue, as seen in Figure 3b. His447, Glu334, and Ser203 residues play a role in the catalytic activity of AChE enzyme. However, many AChE inhibitors inhibit the enzyme by interacting with the peripheral site, just next to the catalytically active site.[65] Compound **4d** inhibited the enzyme by interacting with Trp286 and Tyr341, which are key residues of the peripheral site. The peripheral site contains many hydrophobic amino acid residues. The hydrophobicity tends to allow settling of a compound, including hydrophobic moiety, in the site. The compound exhibits more hydrophobicity due to its isopropylphenyl moiety; therefore, it could constitute a more favorable interaction with key residues. The molecule exhibited similar interactions with many AChE inhibitors.[66–68] Compound **4f** mainly formed a hydrophobic interaction through π–π stacking with Trp231 and Phe329 hydrophobic residues of BChE (Figure 2c). Besides, it directly formed an aromatic hydrogen bond with Tyr332 and indirectly formed hydrogen bonds with Gly117 and Thr120 via a water bridge, as seen in Figure 3c. Trp231 and Tyr332 of the interacting residues are located in the acyl-binding site of BChE enzyme, and the site provides a high selectivity toward the enzyme.[69] Additionally, Košak et al.[69] have indicated that their hit compound is more effective because it has an OMe group. The OMe group may contribute an additional interaction with Trp82,

stabilizing the natural substrate. The compound **4f** is very closely located to the Trp82 residue because of its OMe group. The group has been considered to be more efficient in BChE enzyme inhibition.

3 | CONCLUSION

We aimed to contribute to the studies of the synthesis of the benzoxanthene compound class. Reactions were carried out by boiling the benzaldehyde, and benzaldehydes were substituted with 2-hydroxy-1,4-naphthoquinone and 5,5-dimethylcyclohexane-1,3-dione in a polar solvent such as ethanol using a 10 mol% bismuth triflate catalyst. Furthermore, to carry out the reaction with heteroaromatic aldehydes, compound **9** was synthesized (**4i**) using a thiophene-2-carbaldehyde. Green chemistry was used during the syntheses, using the one-pot method and recycled Bi(OTf)$_3$. Thus, a new development has been introduced in the synthesis of benzoxanthene compounds. The one-pot method was used to contribute to green chemistry during the syntheses by using ethanol as a solvent and recycled Bi(OTf)$_3$. As a result of this study, novel derivatives showed inhibition at the millimolar levels against these enzymes. The newly synthesized compounds were good inhibitors for GST and AChE/BChE enzymes, respectively. Moreover, their potential inhibition mechanisms have been revealed in this study. The results may be useful for designing and synthesizing new metabolic enzyme inhibitors, which may further prove as potential lead candidates for the design of novel drugs to treat some diseases including AD and cancer in the future.

4 | EXPERIMENTAL

4.1 | Chemistry

4.1.1 | General

All reagents and solvents were purchased from Merck, Sigma-Aldrich, and used without any purification. All yields refer to isolated products after purification. Melting points were measured by using the
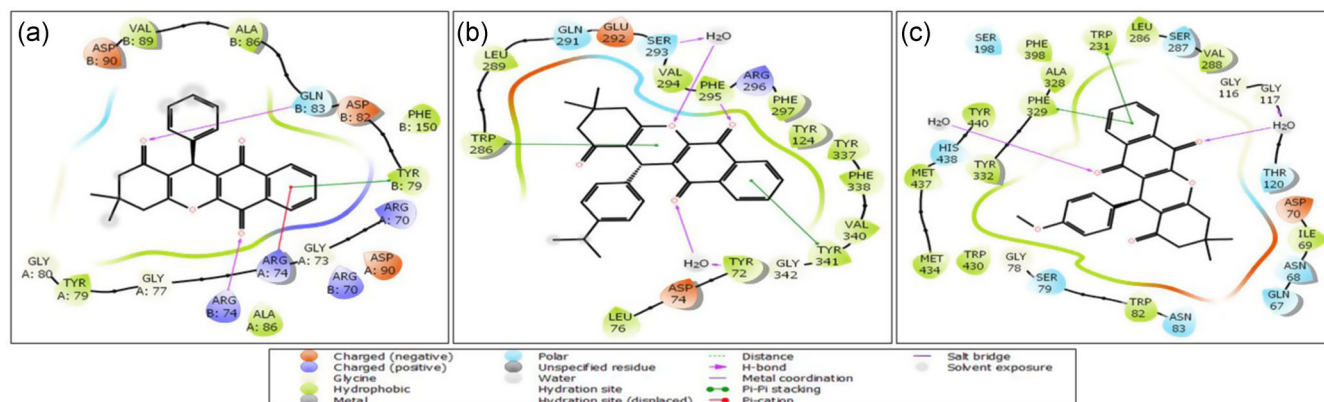
FIGURE 2 A two-dimensional interaction profile between compounds and enzymes; (a) **4a**–GST, (b) **4d**–AChE, and (c) **4f**–BChE. AChE, acetylcholinesterase; BChE, butyrylcholinesterase; GST, glutathione S-transferase
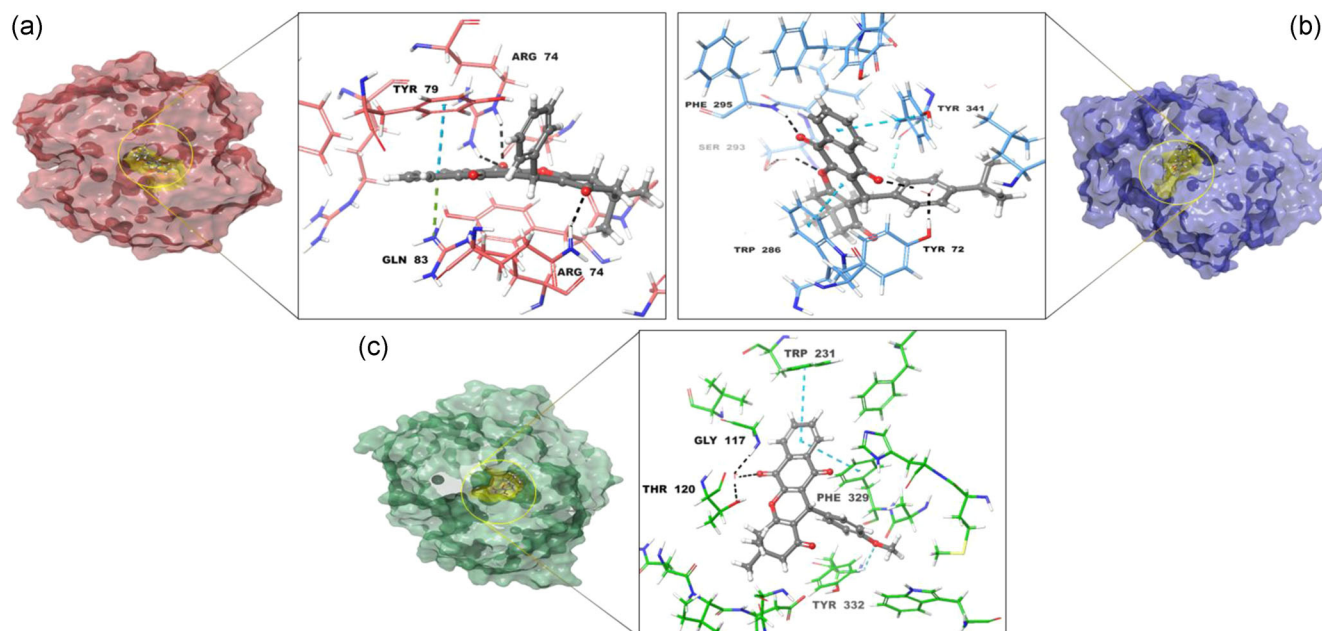
FIGURE 3 A detailed three-dimensional interaction profile between the compounds and the enzymes. (a) **4a**–GST, (b) **4d**–AChE, and (c) **4f**–BChE. Enzyme structures were represented as pink-, blue-, and green-colored surfaces, respectively. Amino acid residues were represented as pink-, blue-, and green-colored thick tube models, respectively. The compounds were represented as gray ball-and-stick model. Hydrogen bond was represented as a black dashed line, π–π stacking interaction was represented as a blue dashed line, π–cation interaction was represented as a green dashed line, and the aromatic hydrogen bond was represented as a turquoise dashed line. AChE, acetylcholinesterase; BChE, butyrylcholinesterase; GST, glutathione S-transferase

capillary tube method with an Electrothermal apparatus. Thermometer correction was not performed. FTIR spectra were obtained on a "PerkinElmer Spectrum One" FTIR spectrometer by attenuated total reflection (ATR) technique. ^{1}H and ^{13}C NMR spectra were determined on a "Bruker AVANCE 500 MHz" spectrometer in dimethyl sulfoxide (DMSO)-d_6. Liquid chromatography–mass spectrometry (LC–MS) spectra were obtained by Agilent 6200 series, TOF/6500 series, and TOF/QTOF mass spectrometer. All the chemicals, including enzymes and other chemicals, used in the experimental procedure were obtained from Sigma-Aldrich Co. (Taufkirchen, Germany).

The InChI codes of the investigated compounds, together with some biological activity data, are provided as Supporting Information Data.

4.1.2 | General procedure for the preparation of compounds 4a–j

A mixture of aromatic aldehyde **1** (1 mmol), 2-hydroxy-1,4-naphthoquinone **2** (1 mmol), dimedone **3** (1 mmol), and a catalytic amount of Bi(OTf)$_3$ (10 mol%) in ethanol (5 ml) was refluxed for the stipulated time at 80°C with a magnetic stirrer. The reaction was terminated by the thin-layer chromatography control of the crude product, as compared with the starting materials. After completion of the reaction, water was added to the mixture and the precipitated solid was filtered and then washed with water and cold ethanol for

separation of the catalyst. The crude product was purified by chromatographic methods.

3,4-Dihydro-3,3-dimethyl-12-phenyl-1H-benzo[b]xanthene-1,6,11-(2H,12H)trione (4a)

C$_{25}$H$_{20}$O$_4$, M$_W$: 384.4239 g/mol (Table 1, entry 1), yellow solid, mp. 263–264°C, yield: 87%. FTIR (ATR) v: 3,028, 2,955, 1,739, 1,660, 1,506, 1,491, 1,374, 813, 764 cm^{-1}. ^{1}H NMR (CDCl$_3$, 500 MHz) δ: 1.05 (3H, s, CH$_3$), 1.14 (3H, s, CH$_3$), 2.24 (1H, d, J = 16.7 Hz, CH$_2$), 2.30 (1H, d, J = 16.3 Hz, CH$_2$), 2.65 (1H, d, J = 17.7 Hz, CH$_2$), 2.73 (1H, d, J = 17.8 Hz, CH$_2$), 5.14 (1H, s, CH), 7.16 (1H, t, J = 7.3 Hz, Ar–H), 7.27 (2H, d, J = 7.4 Hz, Ar–H), 7.39 (2H, d, J = 7.2 Hz, Ar–H), 7.70 (2H, dd, J = 5.7, 3.4 Hz, Ar–H), 8.00 (1H, dd, J = 5.9, 3.1 Hz, Ar–H), 8.13 (1H, dd, J = 6.0, 3.0 Hz, Ar–H) ppm. ^{13}C NMR (CDCl$_3$, 125 MHz) δ: 27.55, 29.26, 32.32, 32.49, 32.93, 32.97, 40.78, 50.71, 114.48, 125.51, 126.63, 126.73, 127.35, 128.65, 128.83, 130.74, 131.84, 133.85, 134.59, 142.57, 149.17, 162.91, 178.10, 183.06, 196.27 ppm. Gas chromatography–mass spectrometry (GC–MS; EI, 70 eV): m/z = 384 (M$^+$).

3,4-Dihydro-3,3-dimethyl-12-(3-nitrophenyl)-1H-benzo[b]xanthene-1,6,11-(2H,12H)trione (4b)

C$_{25}$H$_{19}$NO$_6$, M$_W$: 429.4214 g/mol (Table 1, entry 2), yellow solid, mp. 236–237°C, yield: 88%. FTIR (ATR) v: 3,087 2,960 1,698, 1,666, 1,576, 1,360, 1,322, 809, 749 cm^{-1}. ^{1}H NMR (CDCl$_3$, 500 MHz) δ: 1.12 (3H, s, CH$_3$), 1.19 (3H, s, CH$_3$), 2.28 (1H, d, J = 16.4 Hz, CH$_2$), 2.35 (1H, d, J = 16.4 Hz, CH$_2$), 2.71 (1H, d, J = 17.8 Hz, CH$_2$), 2.80 (1H,

d, J = 17.8 Hz, CH$_2$), 5.09 (1H, s, CH), 7.45 (1H, t, J = 7.9 Hz, Ar–H), 7.63 (2H, td, J = 7.6, 1.1 Hz, Ar–H), 7.79 (2H, td, J = 7.7, 1.3 Hz, Ar–H), 7.93 (1H, d, J = 7.8 Hz, Ar–H), 7.97 (1H, dd, J = 7.8, 1.0 Hz, Ar–H), 8.03 (1H, dd, J = 8.72, 2.3 Hz, Ar–H), 8.06 (1H, brt, J = 2.0 Hz, Ar–H), 8.13 (1H, dd, J = 7.7, 1.1 Hz, Ar–H) ppm. ^{13}C NMR (CDCl$_3$, 125 MHz) δ: 27.67, 29.29, 29.84, 32.64, 32.67, 40.92, 50.74, 114.50, 122.71, 124.87, 129.34, 129.80, 130.12, 132.02, 135.54, 136.21, 144.67, 148.59, 156.64, 162.74, 177.54, 178.26, 196.07 ppm. LC–MS (electrospray ionisation–quadrupole time-of-flight mass spectrometry [ESI–QTOF]): m/z C$_{25}$H$_{19}$NO$_6$ calculated 429.4214, found 430.1287 (M+H).

3,4-Dihydro-3,3-dimethyl-12-(4-fluorophenyl)-1H-benzo[b]-xanthene-1,6,11-(2H,12H)trione (4c)

C$_{25}$H$_{19}$FO$_4$, M$_W$: 402.414 g/mol (Table 1, entry 3), yellow solid, mp. 246–247°C, yield: 92%. FTIR (ATR) ν: 3,000, 2,972, 1,716, 1,651, 1,504, 1,480, 1,376, 1,157, 828, 726 cm^{-1}. ^{1}H NMR (CDCl$_3$, 500 MHz) δ: 1.04 (3H, s, CH$_3$), 1.14 (3H, s, CH$_3$), 2.24 (1H, d, J = 16.3 Hz, CH$_2$), 2.30 (1H, d, J = 16.3 Hz, CH$_2$), 2.65 (1H, d, J = 17.8 Hz, CH$_2$), 2.71 (1H, d, J = 17.8 Hz, CH$_2$), 5.11 (1H, s, CH), 6.93 (2H, t, J = 8.7 Hz, Ar–H), 7.33 (1H, d, J = 8.6 Hz, Ar–H), 7.35 (1H, d, J = 8.6 Hz, Ar–H), 7.71 (2H, dd, J = 5.8, 3.3 Hz, Ar–H), 8.00 (1H, dd, J = 5.7, 3.3 Hz, Ar–H), 8.13 (1H, dd, J = 5.6, 3.3 Hz, Ar–H) ppm. ^{13}C NMR (CDCl$_3$, 125 MHz) δ: 27.54, 29.26, 32.29, 32.33, 32.50, 40.87, 50.84, 114.34, 115.43, 125.20, 126.70, 126.74, 130.37, 130.43, 130.71, 131.75, 133.97, 134.68, 138.59, 149.16, 162.94, 178.01, 183.08, 196.31 ppm. LC–MS (ESI–QTOF): m/z C$_{25}$H$_{19}$FO$_4$ calculated 402.414, found 403.1342 (M+H).

3,4-Dihydro-3,3-dimethyl-12-(4-isopropylphenyl)-1H-benzo[b]-xanthene-1,6,11-(2H,12H)trione (4d)

C$_{28}$H$_{26}$O$_4$, M$_W$: 426.503 g/mol (Table 1, entry 4), yellow solid, mp. 222–224°C, yield: 85%. FTIR (ATR) ν: 3,000, 2,957, 1,660, 1,617, 1,591, 1,378, 1,191 (C–O stretching), 836, 736 cm^{-1}. ^{1}H NMR (CDCl$_3$, 500 MHz) δ: 1.00 (3H, s, CH$_3$), 1.07 (3H, s, CH$_3$), 1.08 (3H, s, CH$_3$), 1.09 (3H, s, CH$_3$), 2.18 (1H, d, J = 16.5 Hz, CH$_2$), 2.23 (1H, d, J = 16.3 Hz, CH$_2$), 2.57 (1H, d, J = 17.7 Hz, CH$_2$), 2.66 (1H, d, J = 17.7 Hz, CH$_2$), 5.04 (1H, s, CH), 7.02 (1H, d, J = 8.2 Hz, Ar–H), 7.20 (2H, d, J = 8.7 Hz, Ar–H), 7.62 (2H, dd, J = 5.8, 3.3 Hz, Ar–H), 7.93 (1H, dd, J = 5.9, 3.1 Hz, Ar–H), 8.05 (1H, dd, J = 5.9, 3.3 Hz, Ar–H) ppm. ^{13}C NMR (CDCl$_3$, 125 MHz) δ: 23.96, 27.68, 27.70, 29.21, 29.22, 32.40, 32.51, 33.76, 33.77, 40.88, 50.88, 114.54, 125.70, 126.59, 126.75, 128.61, 130.72, 131.84, 131.90, 133.81, 134.55, 139.88, 147.76, 149.02, 162.89, 178.18, 183.13, 196.44 ppm. LC–MS (ESI–QTOF): m/z C$_{28}$H$_{26}$O$_4$ calculated 426.503, found 427.187 g/mol (M+H).

3,4-Dihydro-3,3-dimethyl-12-(4-bromophenyl)-1H-benzo[b]-xanthene-1,6,11-(2H,12H)trione (4e)

C$_{25}$H$_{19}$BrO$_4$, M$_W$: 463.3196 g/mol (Table 1, entry 5), yellow solid, mp. 270–271°C, yield: 86%. FTIR (ATR) ν: 3,067, 2,955, 1,660, 1,619, 1,590, 1,466, 1,369, 829, 715 cm^{-1}. ^{1}H NMR (CDCl$_3$, 500 MHz) δ: 1.04 (3H, s, CH$_3$), 1.14 (3H, s, CH$_3$), 2.24 (1H, d, J = 16.4 Hz, CH$_2$), 2.30 (1H, d, J = 16.3 Hz, CH$_2$), 2.65 (1H, d, J = 17.7 Hz, CH$_2$), 2.71 (1H,

d, J = 17.8 Hz, CH$_2$), 5.08 (1H, s, CH), 7.27 (2H, d, J = 8.5 Hz, Ar–H), 7.37 (2H, d, J = 8.5 Hz, Ar–H), 7.72 (2H, dd, J = 5.8, 3.3 Hz, Ar–H), 7.99 (1H, dd, J = 5.9, 3.0 Hz, Ar–H), 8.13 (1H, dd, J = 5.9, 3.0 Hz, Ar–H) ppm. ^{13}C NMR (CDCl$_3$, 125 MHz) δ: 27.51, 27.53, 29.25, 29.27, 32.61, 32.63, 40.85, 50.78, 114.02, 121.35, 124.87, 126.72, 126.74, 130.57, 130.65, 131.68, 131.75, 134.01, 134.72, 141.72, 149.19, 163.06, 177.95, 183.01, 196.28 ppm. LC–MS (ESI–QTOF): m/z C$_{25}$H$_{19}$BrO$_4$ calculated 463.3196, found 465.0517 (M+2H).

3,4-Dihydro-3,3-dimethyl-12-(4-methoxyphenyl)-1H-benzo[b]-xanthene-1,6,11-(2H,12H)trione (4f)

C$_{26}$H$_{22}$O$_5$, M$_W$: 414.4498 g/mol (Table 1, entry 6), brown solid, mp. 241–242°C, yield: 84%. FTIR (ATR) ν: 3,090, 2,933, 1,716, 1,660, 1,589, 1,486, 1,355, 828, 737 cm^{-1}. ^{1}H NMR (CDCl$_3$, 500 MHz) δ: 0.98 (3H, s, CH$_3$), 1.07 (3H, s, CH$_3$), 2.16 (1H, d, J = 16.9 Hz, CH$_2$), 2.22 (1H, d, J = 16.3 Hz, CH$_2$), 2.56 (1H, d, J = 17.8 Hz, CH$_2$), 2.63 (1H, d, J = 17.8 Hz, CH$_2$), 3.65 (3H, s, CH$_3$), 5.01 (1H, s, CH), 6.70 (2H, d, J = 8.8 Hz, Ar–H), 7.20 (2H, d, J = 8.8 Hz, Ar–H), 7.62 (2H, dd, J = 5.8, 3.3 Hz, Ar–H), 7.92 (1H, dd, J = 5.9, 3.1 Hz, Ar–H), 8.05 (1H, dd, J = 5.8, 3.2 Hz, Ar–H) ppm. ^{13}C NMR (CDCl$_3$, 125 MHz) δ: 27.60, 27.63, 29.23, 29.26, 32.10, 32.48, 40.97, 50.97, 55.29, 114.14, 125.67, 126.60, 126.73, 129.87, 129.89, 130.85, 131.96, 133.80, 134.52, 135.01, 149.08, 158.87, 162.68, 178.14, 183.17, 196.26 ppm. LC–MS (ESI–QTOF): m/z C$_{26}$H$_{22}$O$_5$ calculated 414.4498, found 437.1362 (M+Na).

3,4-Dihydro-3,3-dimethyl-12-(2,4-dichlorophenyl)-1H-benzo[b]-xanthene-1,6,11-(2H,12H)trione (4g)

C$_{25}$H$_{18}$Cl$_2$O$_4$, M$_W$: 453.314 g/mol (Table 1 entry 7), yellow solid, mp. 256–257°C, yield: 89%. FTIR (ATR) ν: 3,000, 2,958, 1,666, 1,618, 1,591, 1,470, 1,373, 851, 715 cm^{-1}. ^{1}H NMR (CDCl$_3$, 500 MHz) δ: 1.05 (3H, s, CH$_3$), 1.14 (3H, s, CH$_3$), 2.22 (1H, d, J = 16.2 Hz, CH$_2$), 2.29 (1H, d, J = 16.3 Hz, CH$_2$), 2.63 (1H, d, J = 17.8 Hz, CH$_2$), 2.68 (1H, d, J = 17.9 Hz, CH$_2$), 5.30 (1H, s, CH), 7.18 (1H, dd, J = 8.4, 2.1 Hz, Ar–H), 7.30 (1H, d, J = 2.1 Hz, Ar–H), 7.40 (1H, d, J = 8.4 Hz, Ar–H), 7.72 (2H, dd, J = 5.8, 3.2 Hz, Ar–H), 7.99 (1H, dd, J = 5.8, 3.2 Hz, Ar–H), 8.14 (1H, dd, J = 5.8, 3.2 Hz, Ar–H) ppm. ^{13}C NMR (CDCl$_3$, 125 MHz) δ: 27.76, 27.78, 29.50, 29.52, 32.16, 32.59, 41.07, 51.02, 112.86, 123.40, 127.00, 127.55, 130.45, 130.85, 131.88, 133.76, 134.06, 134.27, 134.98, 135.04, 150.12, 163.83, 178.08, 183.41, 196.67 ppm. LC–MS (ESI–QTOF): m/z C$_{25}$H$_{18}$Cl$_2$O$_4$ calculated 453.3140, found 453.0647 (M+H).

3,4-Dihydro-3,3-dimethyl-12-(2-hydroxy-5-bromophenyl)-1H-benzo[b]xanthene-1,6,11-(2H,12H)trione (4h)

C$_{25}$H$_{19}$BrO$_5$, M$_W$: 479.31936 g/mol (Table 1, entry 8), brown solid, mp. 249–251°C, yield: 81%. FTIR (ATR) ν: 3,210, 2,955, 1,672, 1,631, 1,574, 1,477, 1,362, 814, 728 cm^{-1}. ^{1}H NMR (CDCl$_3$, 500 MHz) δ: 0.96 (3H, s, CH$_3$), 1.04 (3H, s, CH$_3$), 2.03 (1H, d, J = 16.0 Hz, CH$_2$), 2.24 (1H, d, J = 16.0 Hz, CH$_2$), 2.42 (1H, d, J = 17.7 Hz, CH$_2$), 2.54 (1H, d, J = 17.7 Hz, CH$_2$), 5.02 (1H, s, CH), 7.12 (1H, d, J = 2.0 Hz, Ar–H), 7.27 (1H, dd, J = 8.6, 2.4 Hz, Ar–H), 7.37 (1H, dd, J = 8.7, 2.4 Hz, Ar–H), 7.84 (2H, dd, J = 6.9, 2.1 Hz, Ar–H), 7.93 (1H, dd, J = 6.9,

2.1 Hz, Ar–H), 8.03 (1H, dd, J = 6.8, 2.1 Hz, Ar–H) ppm. ^{13}C NMR (CDCl$_3$, 125 MHz) δ: 27.69, 27.74, 29.58, 29.62, 32.36, 32.50, 41.27, 51.12, 115.34, 116.08, 118.33, 121.61, 126.90, 127.87, 129.51, 130.77, 133.46, 134.44, 148.25, 150.55, 164.73, 177.55, 181.80, 195.50 ppm. LC–MS (ESI–QTOF): m/z C$_{25}$H$_{19}$BrO$_5$ calculated 479.3193, found 479.0573 (M+H).

3,4-Dihydro-3,3-dimethyl-12-thienyl-1H-benzo[b]xanthene-1,6,11-(2H,12H)trione (4i)

C$_{23}$H$_{18}$O$_4$S, M$_W$: 390.45162 g/mol. (Table 1, entry 9), yellow solid, mp. 232–233°C, yield: 82%. FTIR (ATR) ν: 3,072, 2,956, 1,659, 1,616, 1,592, 1,468, 1,377, 815, 705 cm^{-1}. ^{1}H NMR (CDCl$_3$, 500 MHz) δ: 1.13 (3H, s, CH$_3$), 1.15 (3H, s, CH$_3$), 2.24 (1H, d, J = 16.7 Hz, CH$_2$), 2.30 (1H, d, J = 16.3 Hz, CH$_2$), 2.64 (1H, d, J = 17.8 Hz, CH$_2$), 2.73 (1H, d, J = 17.8 Hz, CH$_2$), 5.30 (1H, s, CH), 6.86 (1H, dd, J = 5.1, 3.6 Hz, Ar–H), 7.01 (1H, dd, J = 3.5, 0.9 Hz, Ar–H), 7.10 (1H, dd, J = 5.1, 1.1 Hz, Ar–H), 7.73 (2H, dd, J = 7.0, 2.1 Hz, Ar–H), 8.07 (1H, dd, J = 6.9, 2.1 Hz, Ar–H), 8.14 (1H, dd, J = 6.8, 2.2 Hz, Ar–H) ppm. ^{13}C NMR (CDCl$_3$, 125 MHz) δ: 27.33, 27.38, 27.64, 27.66, 29.34, 29.37, 40.88, 50.85, 114.06, 124.57, 126.73, 126.81, 127.22, 130.73, 131.78, 133.98, 134.70, 145.99, 148.94, 163.35, 178.00, 182.96, 196.20 ppm. LC–MS (ESI–QTOF): m/z C$_{23}$H$_{18}$O$_4$S calculated 390.4516, found 391.0988 (M+H).

3,4-Dihydro-3,3-dimethyl-12-(4-benzyloxyphenyl)-1H-benzo[b]-xanthene-1,6,11-(2H,12H)trione (4j)

C$_{32}$H$_{26}$O$_5$, M$_W$: 490.54584 g/mol (Table 1, entry 10), yellow solid, mp. 232–233°C, yield: 82%. FTIR (ATR) ν: 3,089, 3,065, 2,962, 2,935, 1,714, 1,665, 1,585, 1,482, 1,354, 826, 733 cm^{-1}. ^{1}H NMR (CDCl$_3$, 500 MHz) δ: 0.99 (3H, s, CH$_3$), 1.08 (3H, s, CH$_3$), 2.15 (1H, d, J = 16.4 Hz, CH$_2$), 2.20 (1H, d, J = 16.4 Hz, CH$_2$), 2.53 (1H, d, J = 17.7 Hz, CH$_2$), 2.60 (1H, d, J = 17.7 Hz, CH$_2$), 5.09 (1H, s, CH), 5.65 (2H, s, CH$_2$), 6.70 (2H, dd, J = 8.5, 2.1 Hz, Ar–H), 7.27 (2H, dd, J = 8.6, 2.1 Hz, Ar–H), 7.32 (1H, t, J = 7.9 Hz, Ar–H), 7.40 (2H, dd, J = 7.9, 1.9 Hz, Ar–H), 7.51 (2H, d, J = 7.7, 2.2 Hz, Ar–H), 7.62 (2H, dd, J = 5.8, 3.3 Hz, Ar–H), 7.92 (1H, dd, J = 5.9, 3.1 Hz, Ar–H), 8.05 (1H, dd, J = 5.8, 3.2 Hz, Ar–H) ppm. ^{13}C NMR (CDCl$_3$, 125 MHz) δ: 27.50, 27.53, 29.13, 29.16, 32.15, 32.58, 40.87, 50.94, 55.32, 114.24, 126.67, 126.80, 126.93, 127.12, 127.23, 127.66, 128.54, 128,76, 129.77, 129.99, 130.55, 131.76, 133.79, 134.41, 135.13, 136.71, 149.12, 157.66, 161.98, 177.04, 183.01, 195.96 ppm. LC–MS (ESI–QTOF): m/z C$_{23}$H$_{18}$O$_4$S calculated 390.4516, found 391.0988 (M+H).

4.2 | Biochemical studies

4.2.1 | GST activity

The GST activity was measured at 25°C using CDNB as a substrate. The assay system included a phosphate buffer (pH 6.5), GSH (20 mM), and CDNB (25 mM). A spectrophotometer (UV mini 1240; Shimadzu, Japan) was used to estimate the changes in absorbance at 340 nm for 3 min. The inhibitory effects of novel compounds on GST enzyme activity were evaluated by using their different concentrations, similar to the concentration range used in the previous study.[57]

4.2.2 | AChE/BChE activities

The AChE/BChE inhibitory effects of benzo[b]xanthane derivatives was measured according to the method of Ellman et al.,[70] conforming to the previous studies.[71] It was spectrophotometrically measured at 412 nm using acetylthiocholine iodide and butyrylcholine iodide as a substrate in reactions, and 5,5′-dithiobis(2-nitrobenzoic acid) was used to take the activity measurements of AChE and BChE enzymes (Table 3). In the K_i study for these enzymes, 3 separate K_i values were obtained and their averages were calculated, and the standard deviations are presented in Table 3. For IC$_{50}$, the procedure was performed three times, and the averages are presented in Table 3.

4.3 | Molecular docking studies

The possible inhibition mechanism of compounds, which most actively inhibited GSH, AChE, and BChE enzymes, was detected using induced-fit docking method (Small Drug Discovery Suites package, Schrodinger, LLC). Two-dimensional structures of synthesized compounds were sketched and their three-dimensional structures were obtained. The compounds were prepared using the LigPrep module, according to the method described in previous studies.[72,73]

Crystal structures of GST (PDB ID: 5J41), AChE (PDB ID: 4M0E), and BChE (PDB ID: 5NN0) enzymes obtained from RCSB Protein Data Bank were used in molecular docking studies. The structures were chosen due to their high resolution and cocrystallized ligand. Then, the structures were prepared for docking studies with the protein preparation wizard module.[74] The protein preparation was performed according to the method described in previous studies.[75,76] Binding sites of enzymes were predicted using the Sitemap module for detection of catalytically active site and allosteric site.[56] Binding site prediction and evaluation of the sites were performed according to the method described in previous studies.[77] The induced-fit docking method was tested with the redocking process. Following molecular docking studies of most effective compounds were performed using induced-fit docking module.[78]

CONFLICT OF INTERESTS

The authors declare that there are no conflict of interests.

ORCID

Kadir Turhan http://orcid.org/0000-0002-7718-1618
Fikret Türkan http://orcid.org/0000-0002-0538-3157
Halide S. Karaman http://orcid.org/0000-0001-7925-7156

REFERENCES

[1] F. Nemati, S. Sabaqian, *J. Saudi Chem. Soc.* **2017**, *21*, 383. https://doi.org/10.1016/j.jscs.2014.04.009

[2] M. B. Gunjegaonkar, S. A. Fegade, R. C. Kolhe, *Int. J. Res. Phar. Chem.* **2018**, *8*, 319.

[3] H. Singh, B. Nand, J. Sindhu, J. M. Khurana, C. Sharma, K. R. Aneja, *J. Braz. Chem. Soc.* **2014**, *5*, 1178. https://doi.org/10.5935/0103-5053.20140095

[4] U. Kusampally, R. Varala, C. R. Kamatala, S. Abbagoni, *Chem. Data Collect.* **2019**, *20*, 100201. https://doi.org/10.1016/j.cdc.2019.100201

[5] J. Gersmeier, C. Kretzer, S. Di Micco, L. Miek, H. Butschek, V. Cantone, R. Bilancia, R. Rizza, F. Troisi, N. Cardullo, C. Tringali, A. Ialenti, A. Rossi, G. Bifulco, O. Werz, *Biochem. Pharm.* **2019**, *165*, 263. https://doi.org/10.1016/j.bcp.2019.03.003

[6] E. P. Mayoral, E. Soriano, V. Calvino-Casilda, M. L. Rojas-Cervantes, R. M. Martín-Aranda, *Catal. Today* **2017**, *285*, 65. https://doi.org/10.1016/j.cattod.2017.01.048

[7] U. V. Mallavadhani, C. V. Prasad, S. Shrivastava, V. G. M. Naidu, *Eur. J. Med. Chem.* **2014**, *83*, 84. https://doi.org/10.1016/j.ejmech.2014.06.012

[8] B. C. Zorzanelli, L. N. de Queiroz, R. M. A. Santos, L. M. Menezes, F. C. Gomes, V. F. Ferreira, F. Silva, B. K. Robbs, *Future Med. Chem.* **2018**, *10*, 1141. https://doi.org/10.4155/fmc-2017-0205

[9] S. Golmakaniyoon, V. R. Askari, K. Abnous, A. Zarghi, R. Ghodsi, *Iran. J. Pharm. Res.* **2019**, *18*, 16.

[10] H. R. Shaterian, K. Azizi, *Res. Chem. Intermed.* **2015**, *41*, 409. https://doi.org/10.1007/s11164-013-1202-4

[11] J. M. Khurana, A. Chaudhary, A. Lumb, B. Nand, *Green Chem. Lett. Rev.* **2012**, *14*, 2321. https://doi.org/10.1039/c2gc35644a

[12] J. M. Khurana, A. Lumb, A. Chaudhary, B. Nand, *Synth. Commun.* **2013**, *43*, 2147. https://doi.org/10.1080/00397911.2012.688230

[13] B. Maleki, E. Akbarzadeh, S. Babaee, *Dyes Pigm.* **2015**, *23*, 222. https://doi.org/10.1016/j.dyepig.2015.08.009

[14] M. Fathollahi, R. Shahnaz, A. M. Amani, *Comb. Chem. High Throughput Screening* **2018**, *21*, 5. https://doi.org/10.2174/1386207321666180104111508

[15] A. H. Bhatt, V. R. Shah, R. M. Rawal, *Sci. News* **2019**, *118*, 100.

[16] V. Rama, K. Kanagaraj, K. Pitchumani, K., *Tetrahedron Lett.* **2012**, *53*, 1018. https://doi.org/10.1016/j.tetlet.2011.10.143

[17] S. Singh, J. Tiwari, D. Jaiswal, A. K. Sharma, J. Singh, V. Singh, J. Singh, *Curr. Organocatal.* **2018**, *5*, 51. https://doi.org/10.2174/2213337205666180614113032

[18] M. Abd El Aleem, A. Ali El-Remaily, *Chin. J. Catal.* **2015**, *36*, 1124. https://doi.org/10.1016/S1872-2067(14)60308-9

[19] S. Pourshahrestani, I. Mohammadpoor-Baltork, M. Moghadam, S. Tangestaninejad, A. R. Khosropour, V. Mirkhani, *J. Iran. Chem. Soc.* **2015**, *12*, 573. https://doi.org/10.1007/s13738-014-0514-7

[20] H. Mofakham, R. Ghadari, A. Shaabani, M. Pedarpour, S. Ghasemi, *J. Iran. Chem. Soc.* **2013**, *10*, 307. https://doi.org/10.1007/s13738-012-0160-x

[21] J. Li, L. Lu, W. Su, *Tetrahedron Lett.* **2010**, *51*, 2434. https://doi.org/10.1016/j.tetlet.2010.02.149

[22] P. Paliwal, S. R. Jetti, A. Bhatewara, T. Kadre, S. Jain, *Hindawi Org. Chem.* **2013**, 1. https://doi.org/10.1155/2013/197612

[23] Z. N. Tisseh, A. Bazgir, *Dyes Pigm.* **2009**, *83*, 258. https://doi.org/10.1016/j.dyepig.2008.09.003

[24] B. Karami, S. J. Hoseini, K. Eskandari, A. Ghasemi, H. Nasrabadi, *Catal. Sci. Tech.* **2012**, *2*, 331. https://doi.org/10.1039/c1cy00289a

[25] J. Safaei-Ghomi, F. Eshteghal, *Ultrason. Sonochem.* **2017**, *38*, 488. https://doi.org/10.1016/j.ultsonch.2017.03.047

[26] N. G. Khaligh, *Tetrahedron Lett.* **2012**, *53*, 1637. https://doi.org/10.1016/j.tetlet.2012.01.092

[27] M. Pirouzmand, A. M. Gharehbaba, Z. Ghasemi, *J. Mex. Chem. Soc.* **2016**, *60*, 183.

[28] F. K., Behbahani, M. J., Valiallahi, Arab, *J. Chem.* **2017**, *10*, 1686. https://doi.org/10.1016/j.arabjc.2013.06.014

[29] A. Rahmatpour, *Monatsh. Chem.* **2013**, *144*, 1205. https://doi.org/10.1007/s00706-013-0931-9

[30] M. Hajimohammadi, *Iran. J. Catal.* **2016**, *6*, 107.

[31] V. W. Godse, S. S. Rindhe, L. Kotai, P. S. Kendrekar, *Int. J. Org. Chem.* **2017**, *7*, 99. https://doi.org/10.4236/ijoc.2017.72009

[32] A. P. Marjani, A. Abdollahi, M. Ezzati, E. Nemati-Kande, *J. Heterocycl. Chem.* **2017**, *55*, 1324. https://doi.org/10.1002/jhet.3164

[33] K. K. Garlapati, S. S. Babu, N. Srinivasu, T. M. Chavali, *Asian J. Chem.* **2018**, *30*, 804. https://doi.org/10.14233/ajchem.2018.21018

[34] M. F. C. Cardoso, *J. Braz. Chem. Soc.* **2017**, *28*, 1926. https://doi.org/10.21577/0103-5053.20170032

[35] T. Ollevier, *Org. Biomol. Chem.* **2013**, *11*, 2740. https://doi.org/10.1039/C3OB26537D

[36] S. Répichet, A. Zwick, L. Vendier, C. Le Roux, J. Dubac, *Tetrahedron Lett.* **2002**, *43*, 993. https://doi.org/10.1016/S0040-4039(01)02307-3

[37] S. Bhat, R. A. Naikoo, M. A. Mir, R. A. Bhat, M. A. Malla, R. Tomar, *Hindawi J. Mater.* **2016**, *13*, 1. https://doi.org/10.1155/2016/7908584

[38] A. V. S. Reddy, M. V. Reddy, Y. T. Jeong, *Res. Chem. Intermed.* **2016**, *42*, 5209. https://doi.org/10.1007/s11164-015-2350-5

[39] B. Du, G. Cai, B. Zahao, X. Meng, X. Wang, Y. Li, *Res. Chem. Intermed.* **2013**, *39*, 1323. https://doi.org/10.1007/s11164-012-0688-5

[40] H. R. Shaterian, M. Ranjbar, K. Azizi, *J. Mol. Liq.* **2011**, *162*, 95. https://doi.org/10.1016/j.molliq.2011.06.013

[41] M. Dabiri, Z. N. Tisseh, A. Bazgir, *J. Heterocycl. Chem.* **2010**, *47*, 1062. https://doi.org/10.1002/jhet.420

[42] H. R. Shaterian, M. Seghipour, E. Mollashahi, *Res. Chem. Intermed.* **2014**, *40*, 1345. https://doi.org/10.1007/s11164-013-1043-1

[43] F. Türkan, Z. Huyut, P. Taslimi, M. T. Huyut, I. Gülucin, *Drug Chem. Toxicol.* **2018**, *43*, 423. https://doi.org/10.1080/01480545.2018.1497644

[44] N. Balcı, F. Türkan, H. Şakiroğlu, A. Aygün, F. Şen, *Heliyon* **2019**, *5*, e01422. https://doi.org/10.1016/j.heliyon.2019.e01422

[45] F. Türkan, Z. Huyut, Y. Basbugan, I. Gulcin, *Drug Chem. Toxicol.* **2019**, *43*, 27. https://doi.org/10.1080/01480545.2019.1608230

[46] F. Türkan, *Arch. Physiol. Biochem.* **2019**, https://doi.org/10.1080/13813455.2019.1618341.

[47] F. Türkan, A. Aygun, H. Şakiroğlu, F. Sen, *BioNanoScience* **2019**, *9*, 683. https://doi.org/10.1007/s12668-019-00636-w

[48] Y. Temel, M. U. Koçyigit, M. Ş. Taysi, F. Gökalp, M. B. Gürdere, Y. Budak, M. Ceylan, İ. Gulçin, M. Çiftci, *J. Biochem. Mol. Toxicol.* **2018**, *32*, e22034. https://doi.org/10.1002/jbt.22034

[49] i. Gülçin, A. Scozzafava, C. T. Supuran, H. Akıncıoğlu, Z. Koksal, F. Türkan, S. Alwasel, *J. Enzyme Inhib. Med. Chem.* **2016**, *31*, 1095. https://doi.org/10.3109/14756366.2015.1094470

[50] E. Garibov, P. Taslimi, A. Sujayev, Z. Bingöl, S. Çetinkaya, İ. Gulcin, S. Beydemir, V. Farzaliyev, S. H. Alwasel, C. T. Supuran, *J. Enzyme Inhib. Med. Chem.* **2016**, *31*, 1. https://doi.org/10.1080/14756366.2016.1198901

[51] F. Türkan, M. N. Atalar, A. Aras, İ. Gülçin, E. Bursal, *Bioorg. Chem.* **2019**, *94*, 103333. https://doi.org/10.1016/j.bioorg.2019.103333

[52] K. Çetin Çakmak, İ. Gülçin, *Toxicol. Rep.* **2019**, *6*, 1273. https://doi.org/10.1016/j.toxrep.2019.11.003

[53] N. A.E. Al-Sayed, A. E.-S. Farag, M. A. F. Ezzat, H. Akincioglu, İ. Gülçin, S. M. Abou-Seri, *Bioorg. Chem.* **2019**, *93*, 103312. https://doi.org/10.1016/j.bioorg.2019.103312

[54] B. Kuzu, M. Tan, P. Taslimi, İ. Gülçin, M. Taspınar, N. Menges, *Bioorg. Chem.* **2019**, *86*, 187. https://doi.org/10.1016/j.bioorg.2019.01.044

[55] H. E. Aslan, Y. Demir, M. S. Özaslan, F. Türkan, S. Beydemir, O. I. Kufrevioglu, *Drug Chem. Toxicol.* **2018**, *42*, 634. https://doi.org/10.1080/01480545.2018.1463242

[56] SiteMap, Schrödinger, LLC, New York, NY **2020**.

[57] W. H. Habig, M. J. Pabst, W. B. Jakoby, *J. Biol. Chem.* **1974**, *249*, 7130.

[58] T. Ertan-Bolelli, K. Bolelli, Y. Musdal, I. Yildiz, E. Aki-Yalcin, B. Mannervik, I. Yalcin, *Artif. Cells, Nanomed., Biotechnol.* **2018**, *46*, 510.

[59] Y. Musdal, T. Ertan-Bolelli, Bolelli, S. Yilmaz, D. Ceyhan, U. Hegazy, B. Mannervik, Y. Aksoy K, *Turk. J. Biochem.* **2012**, *37*, 431.

[60] T. Ertan-Bolelli, Y. Musdal, K. Bolelli, S. Yilmaz, Y. Aksoy, I. Yildiz, E. Aki-Yalcin, I. Yalcin, *ChemMedChem* **2014**, *9*, 984.

[61] C. A. Lipinski, F. Lombardo, B. W. Dominy, P. J. Feeney, *Adv. Drug Deliv. Rev.* **2001**, *46*, 3. https://doi.org/10.1016/s0169-409x(00)00129-0

[62] A. Sau, F. Pellizzari Tregno, F. Valentino, G. Federici, A. M. Caccuri, *Arch. Biochem. Biophys.* **2010**, *500*, 116. https://doi.org/10.1016/j.abb.2010.05.012

[63] D. Stenberg, A. M. Addalla, B. Mannervik, *Biochem. Biophys. Res. Commun.* **2000**, *271*, 59. https://doi.org/10.1006/bbrc.2000.2579

[64] Y. Huang, S. Misquitta, S. Y. Blond, E. Adams, R. F. Colman, *J. Biol. Chem.* **2008**, *283*, 32880. https://doi.org/10.1074/jbc.m805484200

[65] J. Cheung, E. N. Gary, K. Shiomi, T. L. Rosenberry, *ACS Med. Chem. Lett.* **2013**, *4*, 1091. https://doi.org/10.1021/ml400304w

[66] C. Jang, D. K. Yadav, L. Subedi, R. Venkatesan, A. Venkanna, S. Afzal, E. Lee, J. Yoo, E. Ji, S. Y. Kim, M.-H. Kim, *Sci. Rep.* **2018**, *8*, 14921. https://doi.org/10.1038/s41598-018-33354-6

[67] N. M. Borges, G. R. Sartori, J. F. R. Ribeiro, J. R. Rocha, J. B. L. Martins, C. A. Montanari, R. Gargano, *J. Mol. Model.* **2018**, *24*, 41. https://doi.org/10.1007/s00894-017-3548-9

[68] M. Isik, *Neurochem. Res.* **2019**, *44*, 2147. https://doi.org/10.1007/s11064-019-02852-y

[69] U. Košak, B. Brus, D. Knez, S. Žakelj, J. Trontelj, A. Pišlar, S. Gobec, *J. Med. Chem.* **2017**, *61*, 119. https://doi.org/10.1021/acs.jmedchem.7b01086

[70] G. L. Ellman, K. D. Courtney, V. Andres, R. M. Featherston, *Biochem. Pharmacol.* **1961**, *7*, 88. https://doi.org/10.1016/0006-2952(61)90145-9

[71] İ. Gülçin, A. Z. Tel, A. C. Gören, P. Taslimi, S. Alwasel, *J. Food Meas. Charact.* **2019**, *13*, 2062. https://doi.org/10.1007/s11694-019-00127-2

[72] LigPrep, Schrödinger, LLC, New York, NY **2020**.

[73] S. Burmaoglu, E. Akin-Kazancioglu, R. Kaya, M. Kazancioglu, M. Karaman, O. Algul, I. Gulcin, *J. Mol. Struct.* **2020**, *1208*, 127868. https://doi.org/10.1016/j.molstruc.2020.127868

[74] (a) Protein Preparation Wizard; Epik, Schrödinger, LLC, New York, NY, **2016**; (b) Impact, Schrödinger, LLC, New York, NY, 2016; (c) Prime, Schrödinger, LLC, New York, NY, 2020.

[75] M. Aksoy, M. Karaman, P. Guller, U. Guller, O. I. Kufrevioglu, *Curr. Enzyme Inhib.* **2020**, *15*, 197. https://doi.org/10.2174/1573408016666191231123544

[76] P. Guller, M. Karaman, U. Guller, M. Aksoy, O. I. Kufrevioglu, *J. Biomol. Struct. Dyn.* **2020**, https://doi.org/10.1080/07391102.2020.1738962

[77] R. Kalin, Z. Koksal, P. Kalin, M. Karaman, I. Gulcin, H. Ozdemir, *J. Biochem. Mol. Toxicol.* **2020**, *34*, e22421. https://doi.org/10.1002/jbt.22421

[78] (a) Induced Fit Docking protocol; Glide, Schrödinger, LLC, New York, NY, **2016**; (b) Prime, Schrödinger, LLC, New York, NY, 2020.

SUPPORTING INFORMATION

Additional supporting information may be found online in the Supporting Information section.